Low-loss electron energy loss spectroscopy of VC, NbC and TaC

F. Espinosa-Magaña, R. Martínez-Sánchez, A. Duarte-Moller, and L. González-Hernández

The dielectric properties of commercial VC, NbC and TaC powders were determined by analyzing the low loss region of the EELS spectrum in a transmission electron microscope. From these data, the optical joint density of states (OJDS) was obtained by Kramers-Kronig analysis. As maxima observed in the OJDS spectra are assigned to interband transitions across the energy gap, these spectra can be interpreted on the basis of existing energy-band calculations. Comparison between experimental results and theory shows good agreement.

Keywords: EELS; dielectric function; VC; NbC; TaC; electronic band structure.

Se determinaron las propiedades dieléctricas de polvos comerciales de VC, NbC y TaC analizando la región de bajas energías de espectros de EELS en un microscopio electrónico de transmisión. Con estos datos se obtuvo la densidad óptica de estados (OJDS) mediante el análisis de Kramers-Kronig. Debido a que los máximos observados en los espectros corresponden a transiciones interbanda a través del gap de energía, estos espectros pueden interpretarse sobre la base de cálculos existentes de bandas de energía. La comparación entre los resultados experimentales y la teoría muestran buena concordancia.

Descriptores: EELS; función dieléctrica; VC; NbC; TaC; bandas de energía.

Introduction

The electronic structure of transition metal carbides has been studied for more than two decades, TiC being the most extensively reported [1-6]. These compounds

form a class of very hard materials and they often crystallize in the rock salt structure. They show metallic as well as covalent and ionic properties, which make them interesting for both technical applications and fundamental research. While they exhibit a number of unusual properties, most applications of the transition-metal carbides rely upon their extreme hardness, which are typically found in covalent crystals [7]. It is interesting that properties associated with covalent bonding are found in compounds which display a crystal structure normally associated with ionic bonding.

Electron energy-loss spectroscopy (EELS) is a powerful analytical technique that can be used to obtain information on the structure, bonding and electronic properties of a material [8-14]. The interactions of fast electrons with the specimen result in excitations of electrons into unoccupied energy levels in the conduction band. When a spectrum is obtained by analyzing the energy lost by the incident electrons, the region up to an energy loss of ~50 eV is dominated by collective excitations of valence electrons (plasmon), and by interband transitions. At higher energy losses ionization edges occur due to excitation of core electrons into the conduction band.

In the present work, we have conducted low-energy EELS on commercial VC, NbC, and TaC powders obtaining the complex dielectric function and the optical joint density of states by Kramers-Kronig analysis. A comparison is made with theoretical results based on energy-band structure calculations.

Dielectric theory

The low loss region in an energy loss spectrum (<50 eV) contains information about excitations of outer shell electrons and the electronic structure of the material, which determines its optical properties. The excitations of valence electrons are

dominated by collective excitations (plasmon) and single electron interband transitions. Interband transitions originate from the excitation of electrons in the valence bands to empty states in the conduction bands, so these can be identified as transitions across the energy gap in a band structure model. The plasmon peak position is shifted upward due to excitations below the plasma frequency, and downward due to higher energy excitations.

From the dielectric theory, it is possible to relate the experimental single scattering distribution S(E), to the Energy Loss Function Im(-1/Ɛ), by [15-18]:

$$S(E) = \frac{I_0 t}{\pi a_0 m_0 v^2} Im\left[-\frac{1}{\varepsilon(q,E)}\right] \ln\left[1 + (\beta/\theta_E)^2\right] \quad (1)$$

Where Ɛ (q,E) = $Ɛ_1$ +iE_2 is the complex dielectric function at energy loss E and momentum transfer q, a_0 the Bohr radius, m_0 the electron rest mass, *v* the electron beam velocity, θ the scattering angle, *y* is the relativistic factor, I_0 is the zero loss intensity, t is the specimen thickness, and β is the collection semi-angle.

For small q, Ɛ(q,E) varies very slowly with q, so that it can be replaced by Ɛ(E), which can, in principle, be directly compared with optical measurements.

The real and imaginary pasts of the dielectric function can be obtained from the energy loss function Im(-1/Ɛ), through Karemers-Kroning analysis [8,16,17]

$$Re\left[\frac{1}{\varepsilon(E)}\right] = 1 - \frac{2}{\pi} P \int_0^\infty Im\left[-\frac{1}{\varepsilon(E')}\right] \frac{E' dE'}{E'^2 - E^2} \quad (2)$$

Where P stands for the principal value of the integral.

Theoretically, by measuring the absolute cross-section and the thickness of the sample, we can obtain the value of the energy loss function. However, this approach is usually not practically feasible. In order to obtain the absolute value of the energy loss function, the optical dielectric function at one point is needed to normalize the energy loss spectrum. This can be achieved by using the Kramers-Kronig relations, Eq. (2). In the limit E→0, we can obtain the normalization condition for the energy loss spectrum as

$$Re\left[\frac{1}{\varepsilon(0)}\right] = 1 - \frac{2}{\pi} P \int_0^\infty Im\left[-\frac{1}{\varepsilon(E')}\right] \frac{dE'}{E'} \qquad (3)$$

Solving for Im(-1/Ɛ) in Eq. (1) and integrating gives

$$\int_0^\infty \frac{S(E)}{E \ln\left[1 + (\beta/\theta_E)^2\right]} dE = K \int_0^\infty \frac{Im\left[-1/\varepsilon(E)\right]}{E} dE \quad (4)$$

Here we have defined the normalization factor K, as

$$K = \frac{I_0 t}{\pi a_0 m v^2} \qquad (5)$$

Which can be obtained from experimental.

Replacing the right hand side in Eq. (4) by the expression in Eq. (3), and solving for K, allows us to write.

$$K = \frac{2}{\pi \left\{1 - Re\left[1/\varepsilon(0)\right]\right\}} \int_0^\infty \frac{S(E)}{E \ln\left[1 + (\beta/\theta_E)^2\right]} dE \quad (6)$$

For metals, Re Re[1/Ɛ(0)] = 0, since $Ɛ_1$ and $Ɛ_2$ become very large for E→0. For semiconductors Ɛ is real below the band gap and can be obtained from the refractive index by the relation $Ɛ_1 = n^2$. Finally, by substituting Eq. (6) in Eq. (1) and solving for Im[-1/Ɛ)] gives

$$Im\left[-\frac{1}{\varepsilon(E)}\right] = \frac{S(E)}{K\ln\left[1+(\beta/\theta_E)^2\right]} \qquad (7)$$

Another useful relation, used to check consistency of the data is the f-sum rule

$$\int_0^\infty E\varepsilon_2(E)dE = \frac{\pi}{2}E_p^2 \qquad (8)$$

Where E_p is the free electron plasmon energy (Drude Model), defined as

$$E_p^2 = \frac{\hbar^2 n e^2}{\varepsilon_0 m} \qquad (9)$$

Here n is the total charge density, e the electron charge, m the mass of the electron and $Ɛ_0$ the permittivity of vacuum. Thus, the total integral of $EƐ_2$ is proportional to the number of electrons involved in the transition processes.

To compare the experimental results from EELS with the density of states (DOS) obtained from band theory calculations, we can define the optical joint density of states (OJDS), as [3,19]

$$J_1(E) = \frac{2E\varepsilon_2(E)}{\pi E_p^2} \qquad (10)$$

Where E_p, is the plasmon energy in Drude model.

Experimental

In this work the complex dielectric function of commercial VC, NbC and TaC powders (99% pure) were obtained using a Gatan Parallel Electron Energy Loss Spectrometer (PEELS model 766) attached to a Philips CM-200 transmission electron microscope (TEM). Thin specimens suitable for electron microscopy were prepared by placing clean, dry crushed powders onto commercial holey carbon coated copper grids.

Spectra were taken in diffraction mode with 0.1 eV/ch dispersion, an aperture of 3 mm and a collection semi-angle of 4.9 mrad. As the scattering angle in an EELS experiment can involve momentum transfer, we acquired the spectra using a small collector aperture and a camera length of 360 mm, to measure predominantly optical transitions.

The resolution of the spectra was determined by measuring the full width at half-maximum (FWHM) of the zero-loss peak and this was typically close to 1.3 eV when the TEM was operated at 200 kV.

The EELS spectra were corrected for dark current and readout noise. The channel to channel gain variation was minimized by normalizing the experimental spectrum with independently obtained gain spectrum of the spectrometer.

Results and discussion

Spectra acquired with the PEELS spectrometer were Fourier-Log deconvoluted to have the single scattering distributions S(E), and then normalized with the method previously described to obtain the energy loss function Im(-1/Ɛ). The real and imaginary parts of the dielectric function were obtained, after removing surface loss effects, by Kramers-Kronig Analysis, as described by Egerton [8].

Due to our finite energy resolution (1.3 eV), data below 3 eV are not reliable, so we extrapolated an exponential curve between 0 and 3 eV. As is well known, this is a crucial step, for minor changes in the low loss spectrum produce noticeable variations on ε_1 and ε_2, although the energy loss function and optical joint density of states remain almost unaltered.

As required for normalization, we need the value of $\varepsilon 1$ at low energies (optical frequencies) for VC, NbC, and TaC. However, as we adjusted spectra from zero energy loss in the lower part of the spectrum (0-3 eV), we used $\mathrm{Re}[1/\varepsilon(0)] = 0$, valid for conductors.

The energy loss function and the real and imaginary parts of the dielectric function for VC, NbC, and TaC are shown in Figs. 1(a)-1(c). The dominant feature in all energy loss spectra is the volume plasmon at 22.2, 24.0, and 22.4 eV for VC, NbC and TaC, respectively. We may compare these values to the corresponding free-electron plasma energies calculated from Eq. (9).Taking nine electrons as participating in plasma oscillations in all three compounds (metal 3d and 4s orbitals, and nonmetal 2s and 2p orbitals) we obtain 26.2, 23.3, and 23.7 eV calculated for VC, NbC, and TaC, which agree reasonably well with experimental results, except for VC.

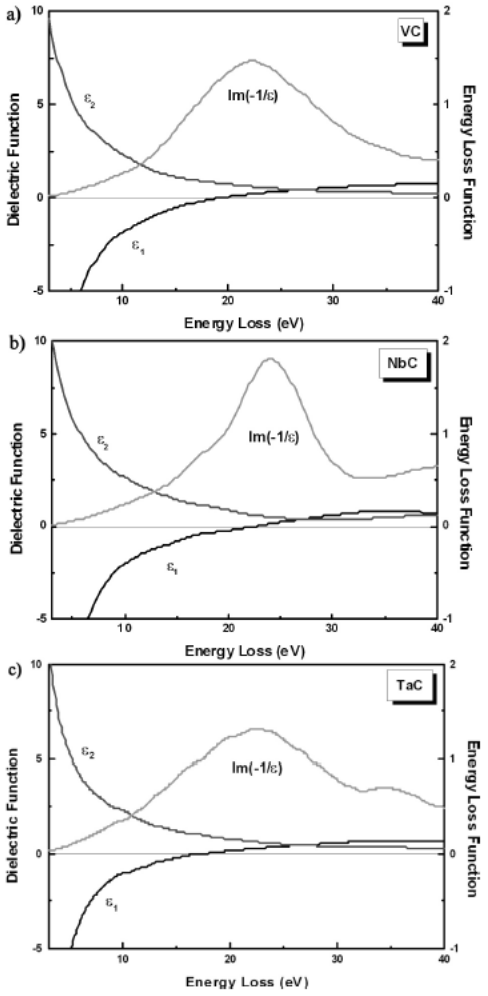

FIGURE 1. Energy Loss Function Im(-1/ε), and real and imaginary parts of the dielectric function ε_1, ε_2 for VC, NbC and TaC.

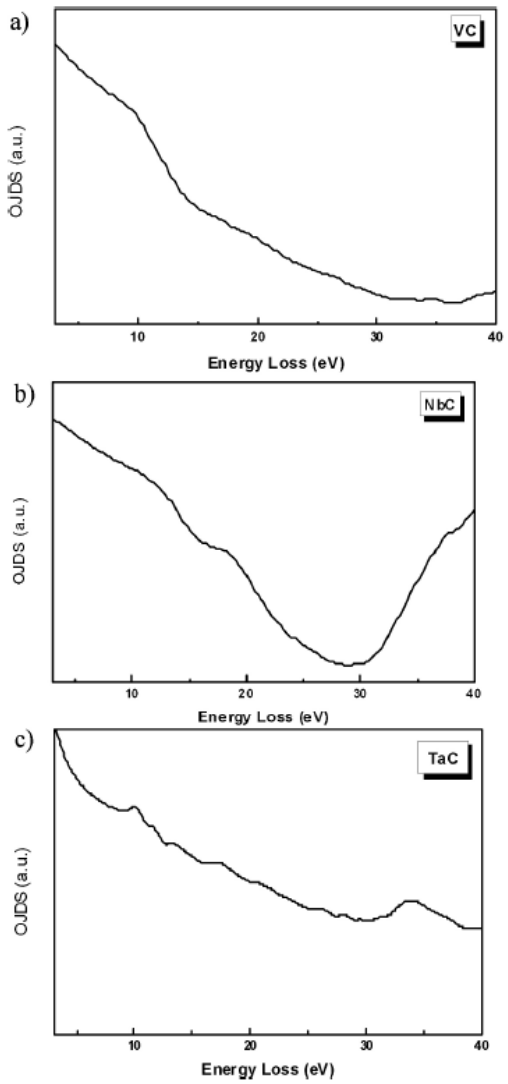

FIGURE 2. Kramers-Kronig derived optical joint density of states $J_1(E)$, for VC, NbC and TaC.

The Ɛ spectra show zero upward crossing at 19.2, 22.4, and 17.0 eV for VC, NbC, and TaC respectively, indicating that the dominant peak in the energy loss spectrum is a well defined plasmon. The absence of any other zero crossing implies that there are no free electrons in these compounds and the peaks appearing at energies below the plasmon peak are effectively due to interband transitions, supporting the analysis made by Pflüger *et al. [3]* for VC. Similar results are expected for NbC and

TaC as these compounds belong to the same transition metal carbides group, all having fcc (NaCl) structure.

TABLE I. Comparison between EELS and theoretical calculations for VC.

EELS (present work)	Theoretical Calculations [20]	Origin
10.0 eV	10.0 eV	$X_1 - X_5'$
12.2 eV	12.2 eV	$L_2' - L_1$
14.0 eV	13.7 eV	$\Gamma_1 - \Gamma_{12}$
15.2 eV	15.0 eV	$L_1 - L_2'$
16.8 eV	16.3 eV	$X_4' - X_1$

TABLE II. Comparison between EELS and theoretical calculations for NbC.

EELS (present work)	Theoretical Calculations [22]	Origin
11.2 eV	11.7 eV	$L_2' - L_3$
13.4 eV	13.5 eV	$L_3 - L_3$
16.0 eV	16.1 eV	$L_1 - L_3$
19.0 eV	18.2 eV	$L_2' - L_3$

TABLE III. Comparison between EELS and theoretical calculations for HfC.

EELS (present work)	Theoretical Calculations [23]	Origin
10.1 eV	9.9 eV	$W_1 - W_1$
11.7 eV	11.9 eV	$L_1 - L_1$
13.4 eV	13.4 eV	$L_2' - L_1$
14.8 eV	14.6 eV	$L_2' - L_2'$
16.2 eV	16.1 eV	$W_2' - W_1$
17.4 eV	17.5 eV	$W_2' - W_2'$
19.0 eV	19.2 eV	$L_2' - L_3$

As peak positions in the energy loss spectrum at low energy losses are strongly influenced by the volume plasmon and the positions of other excitations, the energy loss spectrum cannot be directly associated with interband transitions. However, the imaginary part of the dielectric function can be associated with interband transitions. In Figs. 1(a)-1(c) we can hardly observe a structure in ε_2 spectra, but this structure exists and it can be made evident as we will show below.

Figures 2(a)-2(c) show the optical joint density of states (J_1) versus energy loss for VC, NbC, and TaC, respectively. It is noted that the peaks associated with interband transitions have been enhanced.

As we mentioned above, the form of the single scattering distribution at low energies is critical for the calculation of ε_1 and ε_2 and we would expect this to be

reflected in J_1 (E). However we do not observe any appreciable changes in the optical joint density of states for energies above 3 eV, when

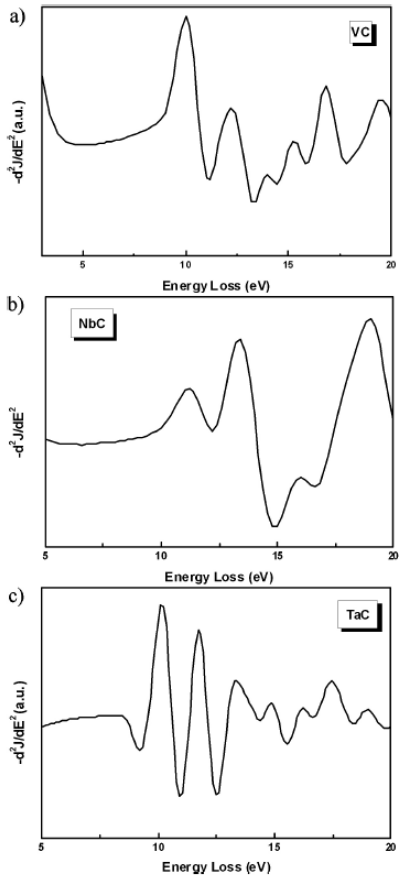

FIGURE 3. Second derivative of J_1(E) with respect to E, for VC, NbC and TaC.

We chose other curves to be adjusted in the range 0-3 eV (e.g. a straight line fitting).

Taking the second derivative of J_1(E) with respect to E, peaks not visible in the J_1(E) Vs E plots are further enhanced, as is shown in Figs. 3(a)-3(c). The appearance and height of these peaks show clearly that they are not noise in character, showing instead more structure associated with interband transitions. For VC, well defined peaks at 10.0, 12.2, 14.0, 15.2, 16.8, and 19.6 eV are observed; for NbC the achieved data show several peaked features at 11.2, 13.4, 16.0, 19.9, eV and for TaC the enhanced peaks appear at 10.1, 11.7, 13.4, 14.8, 16.2, 17.4, and 19.0 eV . As maxima observed

in the $J_1(E)$ vs. E plots are assigned to interband transitions across the energy gap, these peaks can be interpreted on the basis of existing energy-band calculations. Tables I-III show a comparison of our EELS results with theoretical calculations based on the Augmented Plane Wave (APW) method [20].

It must be recalled that, even though we have identified all the peaks in Fig. 3(a)-3(c) with band structure calculations, for many of the structures a unique assignment cannot be made. For example, the peak at 10.0 eV in VC, can arise from transitions of the type $L_1 – L_1$ (9.4 eV), and $L_3– L_3$ (10.6 eV) as well, because of our energy resolution, but in the tables we have chosen the transitions that best fit our experimental results. A more precise assignment could be obtained with experiments carried out with higher energy resolution.

Conclusions

Electronic structure of commercial VC, NbC, and TaC powders were studied by low-loss transmission Electron Energy Loss Spectroscopy. We obtained Kramers-Kronig derived complex dielectric function, and optical joint density of states (OJDS) for the three compounds. Peaks in the OJDS were enhanced by taking the second derivative with respect to energy loss and compared with theoretical predictions based on band-structure calculations for VC, NbC, and TaC. Good agreement was found between our experimental results and those based on theoretical calculations.

The analysis made in this work is an example of the use of EELS to determine electronic structure information, potentially from quite small volumes of material.

References

1. J.L. Calais, Adv. Phys. 26 (1977) 847.

2. D.W. Lynch, C.G. Olson, and D.J. Peterman, Phys. Rev. B 22 (1980) 3991.

3. J. Pfl¨uger, J. Fink, W. Weber, K.P. Bohnen, and G. Crecelins, Phys. Rev. B 30 (1984) 1155.

4. J. Pfl¨uger, J. Fink, W. Weber, K.P. Bohnen, and G. Crecelins, Phys. Rev. B 31 (1985) 1244.

5. V. A. Gubanov, A.L. Ivanovsky, and V.P. Zhukov, Electronic Structure of Refractory Carbides and Nitrides (Cambridge University Press, 1994).

6. A. Cottrell, Chemical Bonding in Transition Metal Carbides, (The Institute of Materials, London, 1995).

7. L.E. Toth, Transition Metal Carbides and Nitrides (Academic Press, New York, 1971).

8. R.F. Egerton, Electron Energy Loss Spectroscopy in the Electron Microscope, 2nd Edition (Plenum Press, New York, 1996).

9. M.M. Disko, C.C. Ahn, and B. Fultz, eds., Transmission Electron Energy Loss Spectrometry in Materials Science, Warrendale (Pennsylvania, 1992).

10. G. Soto, E.C. Samano, R. Machorro, M.H. Far´ıas, and L. Cota-Araiza, Appl. Surf. Sci. 183 (2001) 246.

11. K. van Benthem and C. Els¨asser, J. Appl. Phys. 90 (2001) 6156.

12. K. van Benthem, R.H. French, W. Sigle, C. Els¨asser, and M. Rühle, Ultramicroscopy 86 (2001) 303.

13. G. Brockt and H. Lakner, Micron 31 (2000) 435.

14. S.M. Bose, Phys. Lett. A 289 (2001) 255.

15. R.H. Ritchie, Phys. Rev. 106 (1957) 874.

https://cimav.repositorioinstitucional.mx/jspui/

16. J. Daniels, C.V. Festenberg, H. Raether, and K. Zeppenfeld. Optical Constants of Solids by Electron Spectroscopy. Springer Tracts in Modern Physics, Vol. 54 (Springer Verlag, New York, 1970) p. 78.

17. H. Raether, Excitation of Plasmons and Interband Transitions by Electrons. Springer Tracts in Modern Physics, Vol 88, (Springer-Verlag, New York, 1980).

18. K. Iizumi, K. Saiki, A. Koma, and N.S. Sokolov, J. Electron Spectrosc. and Relat. Phenom. 88 (1998) 457.

19. W.Y. Liang and A.R. Beal, J. Phys. C 9 (1976) 2823.

20. Electronic Structure Database: http://manybody.nrl.navy.mil/esdata/database.html